Hadronic Molecules with Heavy Quarks

Vadim Baru[1,*]

[1]Institut für Theoretische Physik II, Ruhr-Universität Bochum, D-44780 Bochum, Germany

Abstract.
We discuss how to decipher the nature of near-threshold exotic states from experimental line shapes and lattice QCD simulations. A brief overview of the effective-field-theory approach for analyzing such states is presented, highlighting the special role played by the longest-range pion exchange interaction. The method is exemplified through an analysis of the recently discovered doubly-charm state $T_{cc}(3875)^+$.

1 Introduction

In the past two decades, numerous exotic hadronic states have been discovered in the heavy quark sector, challenging conventional quark models [1]. The central theoretical question pertains to the configuration of quarks within these exotic hadrons. One prevalent hypothesis suggests the existence of diquarks and anti-diquarks as compact constituents bearing color charges [2]. Alternatively, exotic states can emerge as bound states of two hadrons, with their size determined by the inverse of the binding momentum [3]. To shed light on this puzzle, one needs to provide theoretically sound distinctions of the different structures and to formulate the appropriate systematic methods for their analysis.

2 Compositeness of exotic states

In the 1960s, Weinberg introduced a method to distinguish between composite (molecular) and elementary (compact) near-threshold bound states in the weak-binding limit [4]. In Ref. [5], it was demonstrated that the same kind of analysis can also be used for unstable exotic states as long as the inelastic threshold is sufficiently remote. The basic idea can be formulated as follows: the probability of a molecular component X in the full wave function of a state is expressable in terms of observables:

$$a = -2\,\frac{X}{1+X}\frac{1}{\gamma} + O(1/\beta), \quad r = -\frac{1-X}{X}\frac{1}{\gamma} + O(1/\beta)\,, \quad g_R^2 = \frac{2\pi\gamma}{\mu^2}X + O(1/\beta)\,, \qquad (1)$$

where a and r represent the scattering length ($a < 0$ indicates bound states) and the effective range, respectively; g_R^2 denotes the physical coupling of a state to the nearby hadronic channel, defined as the residue of the corresponding scattering amplitude at the pole. In the weak binding limit, the binding momentum $\gamma = \sqrt{2\mu E_B}$ (with μ and E_B representing the reduced mass of two hadrons and the binding energy, respectively) is much smaller than the

*e-mail: vadim.baru@tp2.rub.de

typical range of forces, β. This range can be estimated as either the mass of the lightest exchange particle in the hadronic potential or the momentum scale due to the presence of the next higher-energy channel that can couple to the relevant one. It follows from Eq. (1) that

$$X = \sqrt{\frac{1}{1 + 2r/a}} \tag{2}$$

and that in the pure molecular regime ($X \to 1$) $|a| \gg |r|$ and $r \simeq O(\beta^{-1})$, while in the pure compact case ($X \to 0$) $|a| \ll |r|$ and $r < 0$. While these results are valid only for bound states, it was advocated in Ref. [6] that the compositeness should be a continuous function of the parameters in the effective range expansion. The investigation of the pole trajectories and their relation with the compositeness revealed that near-threshold virtual states are of molecular nature while narrow, near-threshold resonances should be interpreted as predominantly compact states. This led to a generalized expression for the compositeness:

$$\bar{X} = \sqrt{\frac{1}{1 + |2r/a|}}, \tag{3}$$

which provides a continuous transition from the regime of bound states to virtual states and resonances. Although the original formula for X was derived under the zero-range approximation, i.e. for $r < 0$, the modified $\bar{X}$ provides reasonable results also for $r > 0$. For example, consider the deuteron, a classical hadronic molecule composed of a proton and a neutron. Experimental values for the scattering length and effective range ($a = -5.41$ fm and $r = +1.75$ fm) point at a predominantly composite nature since $|a| \gg |r|$ and $r > 0$. However, naively using these values in Eq. (2) to evaluate X fails badly resulting in $X \approx 1.7$, as was first pointed out in Ref. [6]. This discrepancy is due to significant range corrections that change the effective range's sign, making the result for the X inapplicable. Instead, applying Eq. (3) yields $\bar{X} = 0.8$, accounting for the natural effect of range corrections and matching with our expectations for this molecular state. Similarly, applying Eq. (3) to the $p - n$ virtual state in the ${}^1S_0$ channel ($a = 23.7$ fm and $r = +2.75$ fm) yields $\bar{X}$ =0.9, completely in line with our expectations.

While a negative effective range in a single-channel case suggests the presence of a substantial compact component, one should be cautious when interpreting a negative effective range in the context of a coupled-channel problem. For example, in a two channel case, the effective range undergoes a negative correction due to the influence of the second channel: [6, 7]

$$\delta r = -\frac{g_2^2}{g_1^2}\sqrt{\frac{\mu_2}{2\mu_1^2\delta_2}}\,, \tag{4}$$

where $g_1(g_2)$ are the couplings of a state to the 1st (2nd) channel, $\mu_1(\mu_2)$ denote the reduced masses of particles in these channels, and δ_2 is the mass difference between the two thresholds. In the special scenario, when the difference between the two thresholds is relatively small, often due to isospin violation, the effective range experiences a particularly pronounced negative adjustment. Prime examples of such states include the $\chi_{c1}(3872)$ and T_{cc}^+, treated as $D^0\bar{D}^{*0}/D^{\pm}\bar{D}^{*\mp}$ and D^0D^{*+}/D^+D^{*0} systems, respectively, where the negative correction δr can reach magnitudes of a few fm. To investigate the nature of states in a coupled-channel scenario, it was suggested in Ref [7] to remove all coupled-channel effects from the effective range and the scattering length, since these effects are of purely hadronic nature, and then employ Eq. (3) for the residual ERE parameters in the dominant channel.

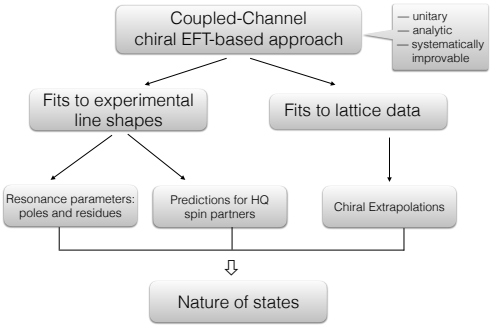

Figure 1. χEFT approach for analysing the properties and nature of exotic states residing near thresholds.

3 Effective Field Theory for near-threshold states

A precondition for understanding the nature of exotic near-threshold states relies on accurately extracting their properties from data. This essential information is typically found in the pole position and residue of a state, which measures its coupling strength to nearby hadronic thresholds. Alternatively, it can be extracted from low-energy hadronic parameters, such as the scattering length and effective range. In experimental analyses, properties of states are often extracted using sums of Breit-Wigner functions, which neglect nearby thresholds and are, therefore, inconsistent with analyticity and unitarity. While this method can confirm the existence of a near-threshold state, it lacks the information needed to fully understand its nature. To address this, systematic theoretical analyses are required to analyze experimental data in a way that respects the principles of analyticity and unitarity. An appropriate framework for this purpose is provided by an Effective Field Theory (EFT) approach, which is model-independent in the relevant energy range for studying near-threshold states. In addition, it allows for the formulation of testable predictions for various observables, where potential molecular candidates and their heavy-quark (HQ) partner states can be observed, see Fig. 1 for an illustration.

The EFT approach is formulated based on an effective Lagrangian consistent with both chiral and heavy-quark spin symmetry (HQSS) of QCD. The key features of the approach can be summarised as follows:

- The coupled-channel hadron-hadron EFT is constructed employing the so-called Weinberg counting [8], proposed originally to treat few-nucleon systems. The potential is constructed to a given order in the chiral expansion Q/Λ_h and then resummed nonperturbatively employing the Lippmann-Schwinger type equations. Simultaneously with the chiral expansion, the potential is expanded around the spin symmetry limit. At leading order, this calls for the inclusion of the spin-partner mass difference together with all interaction vertices constructed in line with HQSS. The binding momenta, the pion mass and the momentum scale generated by the splitting between the open-flavour partner thresholds, which are coupled, (e.g. $B^{(*)}\bar{B}^{(*)}$, $D^{(*)}\bar{D}^{(*)}$, $\Sigma_c^{(*)}\bar{D}^{(*)}$ and so on) are treated as soft scales of the system, generically called Q above; $\Lambda_h \approx 1$ GeV represents the hard scale of the chiral EFT. The explicit inclusion of the coupled-channel scale allows one to extend the energy range where the theory is expected to be applicable, which is especially important for analyzing experimental line shapes.
- Accordingly, at leading order the potential contains the momentum-independent, $\mathcal{O}(Q^0)$, contact interactions, while its long-range contribution stems from the one-pion exchange (OPE). Additionally, to remove the strong regulator dependence resulting from high-momentum contributions arising from S-wave-to-D-wave OPE transitions when multi-

ple open-flavour coupled channels are incorporated, it becomes necessary to introduce the $O(Q^2)$ S-wave-to-D-wave counter term at leading order, as discussed in [9, 10].

- Extension of the approach to the SU(3) sector is straightforward, see e.g. [11].
- The effect of the possible inelastic channels is included by allowing them to couple to the S-wave open-flavour thresholds. As a result, the effective elastic open-flavour potentials acquire imaginary parts driven by unitarity while the contributions to the real parts of the elastic potentials can be absorbed to the redefinition of the momentum-independent $O(Q^0)$ contact interactions.
- All low-energy constants are fixed from a combined fit to the experimental line shapes
- The production operator is typically assumed to proceed via the dominant open-flavour channels, unless there are non-trivial structures in the line shapes, such as a dip close to the threshold. For example, if the cross-section exhibits a dip near the threshold, production may need to occur through more distant inelastic channels, as argued in [12]. Alternatively, such a case may indicate the presence of a Castillejo-Dalitz-Dyson (CDD) zero in the elastic scattering amplitude near the threshold, which would invalidate its effective range expansion [7, 13, 14]. For the role of the triangle singularities, which may also strongly affect the near-threshold line shapes, we refer to the review article [15].

Our very recent applications of this framework include analyses of the experimental line shapes for various near-threshold states: the bottomonium-like states $Z_b(10610)$ and $Z_b(10650)$ [9, 10, 16, 17], the strange charm state $Z_{cs}(3982)$ [18] and the first doubly charmed meson T_{cc} [19, 20] as well as the pentaquark states $P_c(4312)$, $P_c(4440)$ and $P_c(4457)$ [21, 22] and the fully charm tetraquark [23]. These analyses showed consistency of the molecular nature for these states with data and resulted in the predictions for the pole positions and residues of these states and their spin-symmetry partners as well as for the key observables needed for a deeper understanding of the properties and dynamics of these states at various experimental facilities.

4 On the role of the pion exchange

As already pointed out in sec 3, the OPE potential is well defined in the sense of an EFT only in connection with contact operators [24]. Thus, a question typical in phenomenological studies, if the OPE alone provides sufficient binding to generate a shallow state, is not theoretically sound in EFTs. However, the OPE can provide a significant impact on the dynamics and properties of the molecular states, since its inclusion is important to fulfil the correct analytic structure of the hadronic amplitudes. On the one hand, the OPE provides the leading contribution to the left-hand cut of the corresponding scattering amplitude, and thus can affect the ERE parameters. This situation is relevant when the pion can not be on shell, that is, e.g., for $B^{(*)}B^{(*)}$ scattering, NN scattering, $D^{(*)}D^{(*)}$ or $D^{(*)}\bar{D}^{(*)}$ scattering at unphysically large pion masses and so on. Specifically, it was shown in Ref. [20] that the inclusion of the left-hand cut from the OPE is needed for an accurate extraction of the T_{cc} pole from lattice phase shifts for DD^* scattering at $m_\pi = 280$ MeV. On the other hand, if the OPE can go on-shell, the pion, together with two other hadrons in the intermediate state, make up the three-body cut, the appropriate treatment of which is important for studying the decay properties of near-threshold states. Examples of such states include the $T_{cc}(3875)^+$ treated as the DD^* molecule decaying to $DD\pi$; the $\chi_{c1}(3872)$ as the $D\bar{D}^*$ state with the $D\bar{D}\pi$ cut; the P_c states as $\Sigma_c^{(*)}\bar{D}^{(*)}$ with the $\Lambda_c\bar{D}\pi$ cut and so on.

To illustrate the idea, we briefly highlight the results of our recent analysis [19] of the T_{cc} data by LHCb [25, 26]. Among the various exotic candidates, the T_{cc} is particularly intriguing

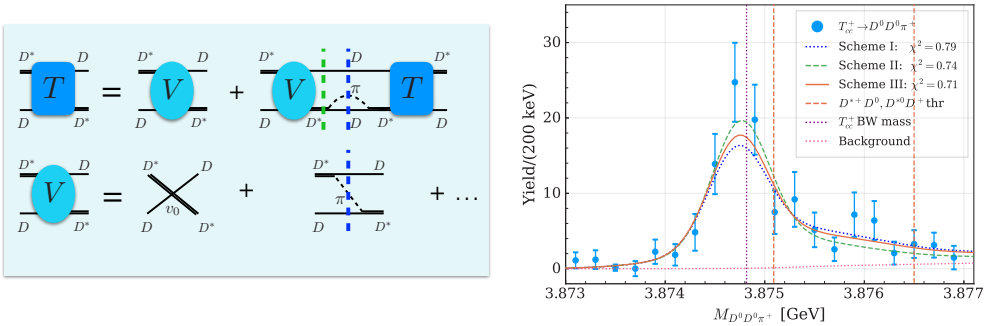

Figure 2. Left panel: the leading order DD^* potential iterated to all order within the scattering equations. Vertical dashed blue and green lines denote the 3-body cut on the real axis and the 2-body cut in the complex plane, respectively. Right panel: the results of our fits to the LHCb data in the $DD\pi$ channel using the potential shown in the left panel; for details of the fits we refer to the original publication [19].

	a [fm]	r [fm]	r' [fm]	$\bar{X}$
scheme III	$\left(-6.72^{+0.36}_{-0.45}\pm 0.27\right) - i\left(0.10^{+0.03}_{-0.03}\pm 0.03\right)$	$-2.40 \pm 0.01 \pm 0.85$	$1.38 \pm 0.01 \pm 0.85$	$0.84 \pm 0.01 \pm 0.06$

Table 1. The S-wave scattering length a and effective range parameters, r and $r' = r - \delta r$ (see Eq. 4), extracted from the best fit as well as the compositeness $\bar{X}$ obtained using Eq. (3).

due to its narrow width, which, except for a small electromagnetic contribution, primarily arises from the strong decay channel $DD\pi$. As a result, the only relevant cut of the amplitude on the real axis is the three-body $DD\pi$ cut, indicated by the vertical blue dashed lines in Fig. 2 (left panel). The results, obtained by explicitly including this cut and iterating to all orders within the Lippmann-Schwinger equations, are displayed in the right panel of Fig. 2 for the $DD\pi$ spectrum (see scheme III). The best fit then yields for the T_{cc} pole $(-356^{+39}_{-38} - i(28 \pm 1))$ keV with respect to the $D^{*+}D^0$ threshold, where the Im part of the pole can be associated with the half width of the T_{cc}. On the other hand, if one neglects three-body effects restricting oneself to the static approximation for the OPE, together with a constant width of the D^*, the half width of the T_{cc} becomes 70 keV, resulting in a severe overestimation. This example shows the importance of the appropriate inclusion of the one-pion exchange and the three body effects for near-threshold states.

The ERE parameters extracted from the best fit (scheme III) are collected in Table 1. The positive effective range r' in the dominant channel, with $|r'| \ll |a|$, and, correspondingly, the compositeness $\bar{X}$ close to 1 both strongly indicate the significant molecular component in the wave function of the T_{cc}.

I would like to thank X. K. Dong, M. L. Du, E. Epelbaum, A. Filin, F. K. Guo, C. Hanhart, A. Nefediev, J. Nieves and Q. Wang for a fruitful and enjoyable collaboration. This work is supported in part by the Deutsche Forschungsgemeinschaft (DFG) through the funds provided to the Sino-German Collaborative Research Center TRR110 "Symmetries and the Emergence of Structure in QCD" (NSFC Grant No. 12070131001, DFG Project-ID 196253076); by BMBF (Contract No. 05P21PCFP1) and by the MKW NRW under the funding code NW21-024-A.

References

[1] N. Brambilla, S. Eidelman, C. Hanhart, A. Nefediev, C. P. Shen, C. E. Thomas, A. Vairo and C. Z. Yuan, Phys. Rept. **873**, 1 (2020)

[2] A. Esposito, A. Pilloni and A. D. Polosa, Phys. Rept. **668** (2017) 1 [arXiv:1611.07920 [hep-ph]].

[3] F.-K. Guo, C. Hanhart, U.-G. Meißner, Q. Wang, Q. Zhao and B.-S. Zou, Rev. Mod. Phys. **90** (2018) 015004 [arXiv:1705.00141 [hep-ph]].

[4] S. Weinberg, Phys. Rev. **1**30 776 (1963)

[5] V. Baru, J. Haidenbauer, C. Hanhart, Y. Kalashnikova and A. E. Kudryavtsev, Phys. Lett. B **586** (2004) 53 [hep-ph/0308129].

[6] I. Matuschek, V. Baru, F. K. Guo and C. Hanhart, Eur. Phys. J. A **57**, no.3, 101 (2021)

[7] V. Baru, X. K. Dong, M. L. Du, A. Filin, F. K. Guo, C. Hanhart, A. Nefediev, J. Nieves and Q. Wang, Phys. Lett. B **833**, 137290 (2022)

[8] S. Weinberg, Phys. Lett. B **251**, 288-292 (1990)

[9] Q. Wang, V. Baru, A. A. Filin, C. Hanhart, A. V. Nefediev and J. L. Wynen, Phys. Rev. D **98**, no.7, 074023 (2018)

[10] V. Baru, E. Epelbaum, A. A. Filin, C. Hanhart, A. V. Nefediev and Q. Wang, Phys. Rev. D **99**, no.9, 094013 (2019)

[11] C. Hidalgo-Duque, J. Nieves and M. P. Valderrama, Phys. Rev. D **87**, no.7, 076006 (2013)

[12] X. K. Dong, F. K. Guo and B. S. Zou, Phys. Rev. Lett. **126**, no.15, 152001 (2021)

[13] V. Baru, C. Hanhart, Y. S. Kalashnikova, A. E. Kudryavtsev and A. V. Nefediev, Eur. Phys. J. A **44**, 93-103 (2010)

[14] X. W. Kang and J. A. Oller, Eur. Phys. J. C **77**, no.6, 399 (2017)

[15] F.-K. Guo, X.-H. Liu and S. Sakai, Prog. Part. Nucl. Phys. **112** (2020) 103757

[16] V. Baru, E. Epelbaum, A. A. Filin, C. Hanhart, R. V. Mizuk, A. V. Nefediev and S. Ropertz, Phys. Rev. D **103**, no.3, 034016 (2021)

[17] V. Baru, E. Epelbaum, A. A. Filin, C. Hanhart and A. V. Nefediev, Phys. Rev. D **107**, no.1, 014027 (2023)

[18] V. Baru, E. Epelbaum, A. A. Filin, C. Hanhart and A. V. Nefediev, Phys. Rev. D **105**, no.3, 034014 (2022)

[19] M. L. Du, V. Baru, X. K. Dong, A. Filin, F. K. Guo, C. Hanhart, A. Nefediev, J. Nieves and Q. Wang, Phys. Rev. D **105**, no.1, 014024 (2022)

[20] M. L. Du, A. Filin, V. Baru, X. K. Dong, E. Epelbaum, F. K. Guo, C. Hanhart, A. Nefediev, J. Nieves and Q. Wang, Phys. Rev. Lett. **131**, no.13, 131903 (2023)

[21] M. L. Du, V. Baru, F. K. Guo, C. Hanhart, U. G. Meißner, J. A. Oller and Q. Wang, Phys. Rev. Lett. **124**, no.7, 072001 (2020)

[22] M. L. Du, V. Baru, F. K. Guo, C. Hanhart, U. G. Meißner, J. A. Oller and Q. Wang, JHEP **08**, 157 (2021)

[23] X. K. Dong, V. Baru, F. K. Guo, C. Hanhart and A. Nefediev, Phys. Rev. Lett. **126**, no.13, 132001 (2021) [erratum: Phys. Rev. Lett. **127**, no.11, 119901 (2021)]

[24] V. Baru, E. Epelbaum, A. A. Filin, F. K. Guo, H. W. Hammer, C. Hanhart, U. G. Meißner and A. V. Nefediev, Phys. Rev. D **91**, no.3, 034002 (2015)

[25] R. Aaij *et al.* [LHCb], Nature Phys. **18**, no.7, 751-754 (2022)

[26] R. Aaij *et al.* [LHCb], Nature Commun. **13**, no.1, 3351 (2022)